30th International Workshop on Water Waves and Floating Bodies, Bristol (UK), 12–15 April, 2015

Forced heaving motion of a floating air-filled bag

John Chaplin & Francis Farley
University of Southampton,
Southampton SO17 1BJ, UK

Adi Kurniawan, Deborah Greaves & Martyn Hann
Plymouth University
Plymouth PL4 8AA, UK

Email: *j.r.chaplin@soton.ac.uk*

Highlights

- Measurements of heaving motions of a floating air-filled bag caused by forced oscillations of the internal pressure.
- Partial validation of a linear frequency-domain numerical model.

1. Introduction

A proposed wave energy converter related to that described by Farley (2011) consists of a pressurised axi-symmretic air-filled bag, ballasted to float at about half depth. The bag contracts and expands under the action of wave-induced heaving motion, pumping air into and out of a secondary, rigid, chamber (V2 in figure 1(a)) which acts as an air spring. The system's resonant frequency in heave is determined largely by V2 and the volume of the bag V1. Oscillating air flow between V1 and V2 drives a power take-off.

This paper describes experiments and numerical modelling aimed at understanding the behaviour of this device. Rather than test it in waves, in this initial investigation we chose to replace the power take-off with an oscillating air pump. Forcing air into and out of the bag periodically caused it to heave and radiate waves when floating in water initially at rest. Measurements of the bag's response are compared with the predictions of a linear frequency-domain radiation theory, which uses a finite difference approach to model the harmonic deformations of the bag. Agreement is promising on the whole, providing some insights into the likely performance of the device when operating as a wave energy converter.

2. Experimental arrangements

The experiments were carried out in the wave basin at Plymouth University, measuring 35m x 15.5m, with a water depth of 3m. The overall height of the bag and ballast container (sketched in fig. 1(b)) was about 1.6m. Since the compressibility of air is the same as in the prototype, the volumes of V1 and V2 had to be considerably larger than those implied by the cube of the scale factor (about 1:16), in order for the resonant frequency to be scaled correctly. Accordingly, V1 was augmented by the volume of an additional air chamber which was connected to the top of the bag by a 100mm diameter flexible hose, and to a similar chamber representing V2, as sketched in figure 1(b). Both chambers were mounted on the gantry spanning the tank, and each had a volume of $1m^3$. The duct between them housed an oscillating air pump.

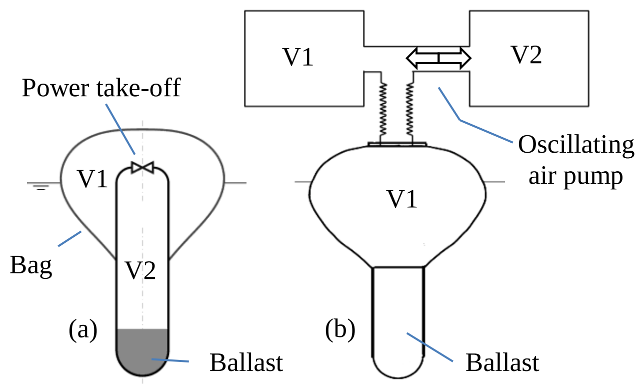

Figure 1 (a) Configuration of (a) the full-scale device and (b) the laboratory model.

The form of construction of the bag, both for the model and envisaged for the full-scale device, is that of a membrane enclosed within an array of longitudinally very stiff tendons distributed around the circumference. This gives it the appearance of a pumpkin, with the membrane bulging out between the tendons, which are intended to carry all of the meridional load. In the model the membrane was unreinforced polyurethane film and the 16 tendons, welded on, were made from 30mm wide polyurethane-coated polyester strips. Ballast was provided by lead shot inside a cylindrical steel container with a hemispherical base, mounted beneath the bag. The device is shown in figure 2, floating in the tank.

The air pump consisted of two pairs of 300mm diameter bellows on either side of diaphragms which were driven by electro-magnetic digital linear actuators. A sketch is shown in figure 3. Other instrumentation included pressure transducers in the bag and on either side of the air pump, and a displacement transducer recording the elevation of the top of the bag. Video cameras recorded the motion of the bag from the side, both above and under water.

Figure 2. Combined under- and above-water images of the bag and ballast container.

Driving the air pump generated an oscillating air flow into and out of the bag, causing it to heave and radiate waves. Measurements were made over a range of frequencies in each of five conditions defined by the initial pressure in the bag and its elevation. As discussed by Kurniawan *et al.* (2015), for a given internal pressure there are in general two elevations at which the bag is in equilibrium in still water.

3. Linear frequency domain numerical model

For the purpose of computing the response of the model device to an oscillating air flow, the shape of a tendon in the vertical plane, together with the outline of the ballast container, can be represented by a series of straight elements of uniform length h between nodes. Nodes and elements are numbered from the bottom of the ballast container to the top of the bag on its axis. (The inlet pipe at the top is omitted.) In still water conditions, the inclination of the nth element from the horizontal is Ψ_n.

Resolving forces in the normal direction at the nth node on the bag (where the radius and the elevation relative to the water surface are R_n and Z_n) leads to

$$\pi R_n \left(P + \rho g H_n Z_n \right) h = T \tan \tfrac{1}{2} \left(\Psi_n - \Psi_{n-1} \right), \qquad (1)$$

assuming that all loads are carried by the tendons. In equation (1) P is the internal pressure, T is the total tension in all tendons, and H_n = 1 when $Z_n < 0$, otherwise 0. Resolving forces at the node at the bottom where the tendon joins the top of the ballast container (n = 1) provides one boundary condition, namely $T \sin \Psi_1 = W + \pi R^2 P$, where W is the submerged weight of the ballast, while at the top (n = N), $\Psi_{N-1} = \pi$ by symmetry. Solutions to equation (1) for the shape of the bag in still water can be found by various means (Kurniawan *et al.*, 2015).

In solving the dynamic case, the time dependent nature of each parameter is represented by a small harmonic perturbation about the mean, i.e. the static solution. Thus the radius of the nth node becomes the real part of $R_n + r_n e^{-i\omega\tau}$ where r_n is a complex amplitude, ω is the frequency and τ is time. Similar adjustments are made to elevations: $Z_n + z_n e^{-i\omega\tau}$; inclinations, $\Psi_n + \psi_n e^{-i\omega\tau}$; the tension, $T + te^{-i\omega\tau}$; the internal pressure, $P + pe^{-i\omega\tau}$, and the internal volume of the bag $V + ve^{-i\omega\tau}$. Also, beneath the water surface all surfaces experience hydrodynamic pressure whose complex amplitude is denoted φ_n.

The solution procedure is first to introduce these perturbations into equation (1), expand the result, discard terms involving products of small quantities, and subtract the static solution in the usual way. It is helpful to define

$$R_n' = R_{n+1} - R_n; \quad Z_n' = Z_{n+1} - Z_n; \quad r_n' = r_{n+1} - r_n; \quad z_n' = z_{n+1} - z_n, \quad n = 1, 2, \ldots N\!-\!1. \qquad (2)$$

The elements of the column matrix $\{r'\} = \{r_1{}' \;\; r_2{}' \;\; \ldots \;\; r_{N\text{-}2}{}'\}^{\mathrm{T}}$ and z_1, the complex amplitude of the heaving motion of the ballast, become the primary unknowns. To a first approximation all other parameters can be expressed in terms of these, ultimately rendering the problem in the form of a set of complex linear equations. Besides the geometry of the system in still water, the other independent parameters are the volume swept out by the air pump, and its frequency ω.

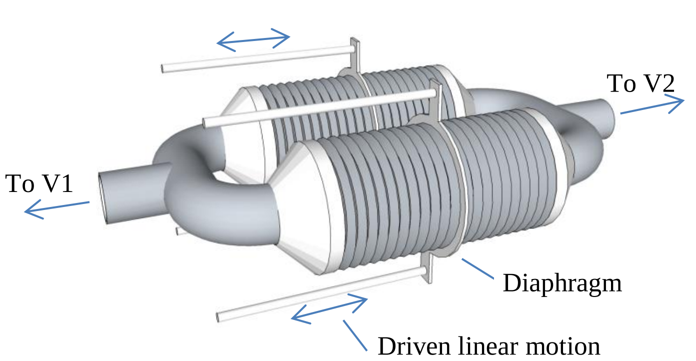

Figure 3. The oscillating air pump.

Hydrodynamic pressures are computed by using an approach for calculating wave radiation by axisymmetric bodies set out by e.g. Fenton (1978) and Isaacson (1982) (both of which contain significant errors). For a given geometry and a given set of normal velocities $\{\upsilon\}$ at the nodes, the result can always be expressed in the form $\{\varphi\} = [D]\{\upsilon\}$. In the present case the elements of [D] are computed from the known initial geometry of the device, and those of $\{\upsilon\}$ can be related to $\{r'\}$ and z_1 by way of the complex amplitude of the internal pressure, which is assumed to follow the adiabatic law in response to the oscillatory flow of air from the air pump.

4. Measurements and predictions

Slow inflation and deflation

Figure 4 shows a plot (as a continuous grey line) of the measured trajectory traced out by the elevation of the top of the bag against its internal pressure, as the bag is slowly inflated in still water. As described by Kurniawan *et al.* (2015), the pressure initially falls as the bag rises, then increases again as the membrane tightens. The trajectory returns along almost the same path as the air is released again. A dashed line represents a numerical solution of equation (1) for these quasi-static conditions. Better agreement with the measurements than that shown by Kurniawan *et al.* has been achieved here by empirically increasing the length of the tendons in the numerical model from 1.5m (as they were when unstressed in the laboratory model) to 1.65m. Of this 150mm difference, about 35mm can be attributed to stretch in the 16 tendons which, over the range of the test conditions, would have been under a tension of at least 300N each. The remaining difference is tentatively associated with the actual inflated form of the membrane. The bag was constructed from 16 'petals' welded together at the tendons. Since the petals were two-dimensional and less stiff under tension than the tendons, it is inevitable that when the bag was inflated, they would bulge out, stretching in both directions and taking some of the load away from the tendons. With this in mind it seems reasonable to argue that the effective tendon length should be increased to reflect the greater meridional length of the bulging and load-carrying membrane. Accordingly, results presented below were computed for a tendon length of 1.65m. Also, amid some uncertainty (within a range of about 8%) about the effective submerged ballast weight, the calculations used a figure of 3659N to provide a reasonable fit with the measurements.

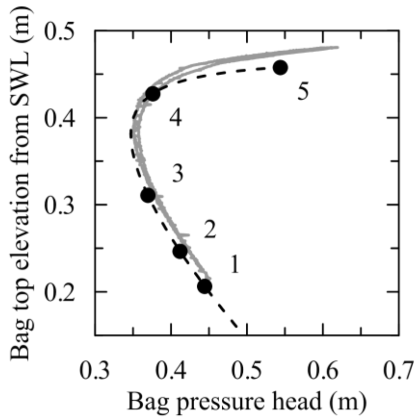

Figure 4. Trajectories of the elevation of the top of the bag when inflated and deflated slowly in still water. The grey line is the measurement, the broken line the prediction, using a tendon length of 1.65m. Initial conditions for dynamic tests are identified 1–5.

Initial conditions for the wave radiation tests and predictions are identified 1–5 in figure 4.

Computed resonant frequencies

Behind the concept of this device lay the idea that the negative stiffness of a body that shrinks as it sinks and expands as it rises in water otherwise at rest would cause it to have a longer resonant period in heave than a rigid body of the same size and shape. This might be an advantage, leading to a reduction in the size of a wave energy converter designed for a given sea-state. Computed resonant periods for compressible and rigid bodies having the shape of defined by the initial conditions in the 5 test cases are plotted in figure 5. For the compressible air-filled bag, predicted periods are more than 15% longer than those for rigid bodies of the same shape, though obviously the frequency response of the bag depends on the stiffness of the air spring, and therefore the volume of air enclosed, and connected to it.

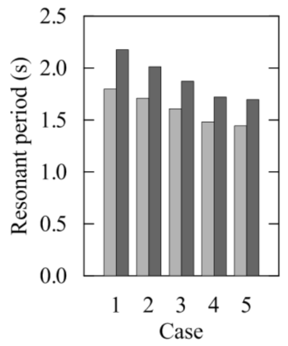

Figure 5. Resonant heave periods of the air-filled bag driven with the air pump (dark grey), and of a rigid body of the same initial shape (light grey).

Response of the device to an oscillating air flow

In these tests the air pump was operated over a range of frequencies in turn, at amplitudes that generated a small heaving motion in the device. Results are plotted below as a function of the period of the driving motion. On the left figure 6 shows, for each case, the amplitude of the vertical motion of the top of the bag, and on the right its phase relative to that of the air pump.

Computed amplitudes and phases agree reasonably well with the measurements for those cases, 5 and 4, in which the bag is strongly inflated and high in the water. The difference between measured and predicted resonant frequencies becomes more pronounced in cases 3, 2 and 1. In the last of these the pressure drop across the membrane would have been negative in the lower part of the bag so that its profile would be concave, but the reason for the disagreement is not clear. Nevertheless, the present numerical model seems to be a good starting point for an investigation into the performance of the device as a wave energy converter.

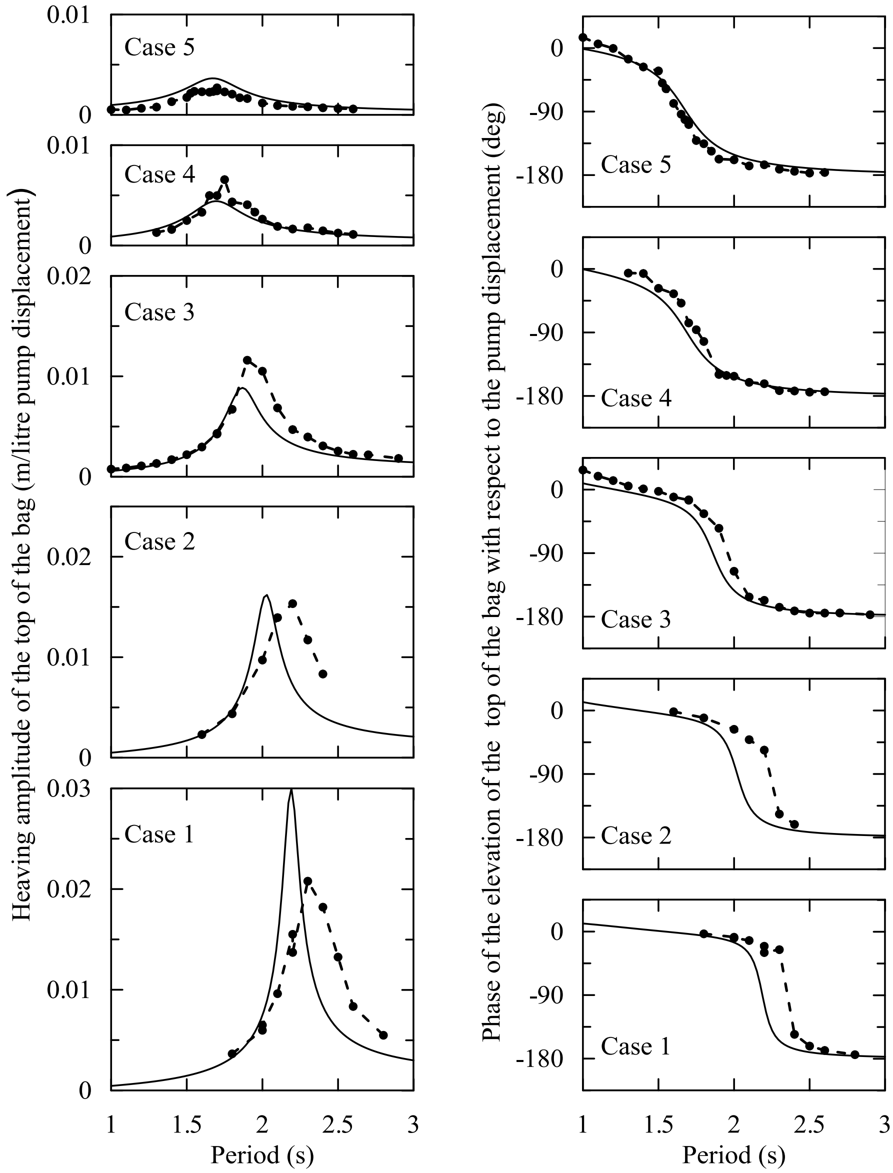

Figure 6. On the left, measured and computed heaving amplitudes of the top of the bag as functions of excitation period for a constant pump displacement of 1 litre. The phase of the motion related to that of the air pump is shown on the right. Measurements are shown as points and broken lines, numerical predictions as continuous lines.

Acknowledgement

This work is supported by the UK EPSRC SuperGen Marine Energy Research Consortium, through grant EP/K012177. We are grateful to Malcolm Cox of Griffon Hoverwork Ltd for supplying model test bags and for useful discussions.

References

Farley, F. J. M. (2011), ‘The free floating clam–a new wave energy converter,’ in Proceedings of the 9th European Wave and Tidal Energy, Southampton, UK

Fenton, J.D. (1978) ‘Wave forces on vertical bodies of revolution’, Journal of Fluid Mechanics, **85**, 241-255.

Isaacson, M. de St Q. (1982) ‘Fixed and floating axisymmetric structures in waves’, Journal of Waterway, Port, Coastal and Ocean Division, Proceedings of the ASCE, **108**, 180-199.

Kurniawan, A., Greaves, D., Hann, M., Chaplin, J.R. & Farley, F.J.M. (2015) ‘Static shapes of a floating inflated bag for wave energy conversion’. Abstract submitted for the 30th International Workshop on Water Waves and Floating Bodies, Bristol, UK.